77th IIW Annual Assembly and International Conference on Welding and Joining 7-12 July 2024 Rhodes, Greece

Comparison of mechanical and microstructural properties by heat source of laser-arc hybrid welding using Aluminum alloys

Seonghyun Kim[1, 2], and *Changwook* Ji[2*]

[1]Department of Materials Science and Engineering, Pusan national University, Busan 46241, South Korea
[2]Smart Forming Process R&D Group, Korea Institute of Industrial Technology, 44776 Ulsan, South Korea

Abstract. High-strength aluminum alloy is attracting attention as a key material for strengthening carbon emission regulations and reducing the weight of vehicle parts to improve fuel efficiency, and the development of welding method to apply it is necessary. However, the high thermal conductivity of aluminum alloy and the presence of an oxide film require high energy density heat input, and it is difficult to secure neat welds and mechanical properties due to limited penetration depth. To address this issue, we attempted to realize high-efficiency and high-quality welding by developing laser-arc hybrid welding. However, optimization to secure neat welds according to the output parameters of the ARM (Adjustable Ring Mode) laser and arc heat source is insufficient. Therefore, this study aimed to investigate the effects of heat input parameters (laser mode, arc current) on weld bead and weld zone quality in laser-arc hybrid welding of aluminum AA6N01-T5, a material commonly used in vehicle parts. We observed the formation of weld bead and weld zone according to the melting and solidification phenomena induced by the mode of ARM lasers and arc sources. Furthermore, analysis was conducted on the mechanical properties and microstructures of the arc-dominated zone and laser-dominated zone.

1 Introduction

Recently, due to the intensification of international environmental regulations to combat global warming, there has been a growing interest in reducing greenhouse gas emissions and improving fuel efficiency in the transportation industry. As a result, the pace of technological development for creating components and manufacturing processes related to high fuel efficiency and emission-free transportation devices is accelerating. Specifically, in the automotive industry, there is ongoing development of materials and component production technologies for eco-friendly vehicles designed to achieve high fuel efficiency. This includes the thinning of steel materials or the application of non-ferrous materials like aluminum, magnesium, and titanium in car bodies[1]. Aluminum is a widely used structural material with low density, high specific strength, good processability, excellent corrosion resistance, and low-temperature characteristics. However, the welding technology required to assemble components using aluminum alloy materials faces challenges due to high thermal and electrical conductivity, as well as the presence of oxide film with a high melting point (2,060 ℃). This necessitates intense heating and makes it difficult to achieve uniform welding quality[1-5]. First, arc welding is one of the most widely used welding techniques due to its low investment and operational costs and efficient joining. When applying arc welding to aluminum materials, the high heat input results in a wide heat-affected zone and the low energy density causes low weld penetration, which can lead to deformations. However, the use of DCEP (Direct Current Straight Positive) welding removes the oxide film, improving weld quality. Additionally, using filler material can result in high welding efficiency and effective gap bridging[6, 7]. When using arc welding methods, issues related to weld quality such as thermal deformation, insufficient penetration, high-temperature cracking, and internal pore formation can occur. Laser welding is a more expensive option, but it offers the benefit of fast welding speeds and minimized weld area due to keyholes, resulting in high-quality welds. When applying laser welding to aluminum materials, although the high reflectivity of the laser reduces weldability and its gap-bridging capability is weak, the method does result in less deformation, deeper penetration due to keyhole formation from the high energy density, and narrower beads. Furthermore, laser welding can be performed at speeds about ten times faster than arc welding[5-7]. Laser welding techniques can lead to issues such as high-temperature cracking, underfill, and internal pore formation or defects due to rapid cooling and solidification[8, 9]. Defects arising in arc welding and laser welding are influenced not only by alloy composition but also by various process variables, either singly or in combination. These defects significantly impact mechanical properties like tensile strength and fatigue strength of the weld. As the porosity within the weld increases, mechanical properties such as tensile strength and fatigue strength drastically decline[10, 11]. Laser-arc hybrid welding combines the high-density, low-heat input of the laser with the low-density, high-heat input of the arc to mutually compensate for the drawbacks and maximize the advantages of each, leading to improved weld quality and speed in aluminum alloys. Due to the characteristics of aluminum materials, active research is underway to optimize laser-arc hybrid welding processes and ensure quality. In

* Corresponding author: cwji@kitech.re.kr

hybrid welding, research is being conducted on synergy effects to ensure the quality of welds, and it is being revealed how the interaction between laser and arc has a positive effect on welds[12]. Additionally, research on the correlation between microstructure and mechanical properties of hybrid welds is actively being conducted[13, 14]. However, there is a lack of research on hybrid welding using ARM laser. Therefore, a study was conducted on the correlation between microstructure and mechanical properties of ARM laser's dual beam, core beam, and ring beam.

2 Experimental materials and methods

AA6N01-T5 Al extrusion alloy plates with dimension 200 x 100 x 5 mm^3 and ER4043 Al filler metal with 1.2 mm diameter were used for welding, whose chemical compositions are shown in Table 1.

Material		Chemical composition (wt%)										
		Si	Mg	Zn	Fe	Ni	Ti	Sr	Cu	Mn	Cr	Al
Base metal	AA6N01-T5 (5t)	0.58	0.96	0.02	0.41	–	0.04	–	0.28	0.03	0.23	Bal.
Filer metal	AX-4043 (1.2 mm)	Si	Mg	Zn	Fe	Ni	Ti	Be	Cu	Mn	Cr	Al
		4.5-6.0	0.05	0.10	0.8	–	0.2	0.0003	0.30	0.05	–	Bal.

Table. 1 Chemical composition of materials

Bead-on-plate experiments of ARM(Adjustable Ring Mode) laser-arc hybrid welding (ARM-LAHW) were carried out. As shown in the Fig. 1, the ARM-LAHW system composed of a HighLight FL-ARM 6000 fiber laser (6kW maximum output power), HIGHYAG BIMO welding head, FRONIUS TPS5000 MIG arc welder, and KUKA KR 60 HA robot.

Fig. 1 ARM laser-arc hybrid welding experimental equipment.

The fiber laser with adjustable ring mode were conducted using a Coherent ARM fiber laser. The laser beam was evenly divided between the core and ring beams. Laser beam with a wavelength of 1064nm were transmitted through an optical fiber with a core diameter of 70 μm and a ring diameter of 180 μm. The collimation system installed on the Precitec YW50 laser head consists of a collimating lens with a focal length of 150 mm and a focal lens with a focal length of 500 mm. The angle between arc torch and the workpiece was 60°. The angle between laser head and the workpiece was 83°. The distance between laser and arc (D_{LA}) was 2mm and the wire extension was 15mm. The high purity argon (99.999%) was used as shielding gas (flow rate was 20L/min). The schematic diagram of the ARM laser-arc hybrid welding experimental setup are shown in Fig. 2.

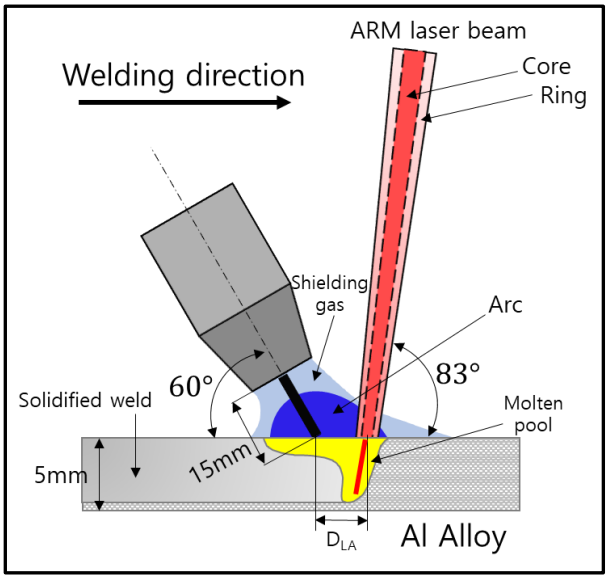

Fig. 2 Schematic diagram of ARM laser-arc hybrid welding.

Detail welding parameters are listed in Table 2.

Parameter	Value
Laser Power	**2 - 4 kW**
Welding speed	**1.5 m/min**
Defocused distance	**0mm**
Focal length	**250mm**
Arc current	**110A**

Table. 2 Welding parameters

After the welding, optical microscopy (OM) and scanning electron microscope (SEM) were conducted to see the microstructure of each. Samples were mechanically ground and polished by abrasive silicon carbide paper (#180 to 1200). Chemical etching was conducted using a modified keller reagent (175ml distilled water + 20ml nitric acid + 3ml hydrogen chloride + 2ml hydrogen fluoride) for 10-20s. And the samples were prepared by the steps with mechanical grinding and polishing using OP-S, and cleaned with ethanol for the electron backscatter diffraction (EBSD) analysis. The EBSD analysis was performed under the step size of 10 μm and the magnification of x150. The analysis of the EBSD results were done using TSL orientation imaging microscopy analysis software. The

micro Vickers hardness test was conducted with a load of 500gf and dwell time of 15s.

3 Results and discussion

3.1 Microstructure

Fig. 3 show the cross-sectional macrostructure of the whole welded joints obtained by dual beam hybrid and core beam hybrid processes, it also shows the microstructure of the weld fusion line and center of each process. In both processes, columnar zone appeared at the weld fusion line and equiaxed zone was observed at the center of the weld. Finer grains were observed in the core beam hybrid welding than in the dual beam hybrid welding.

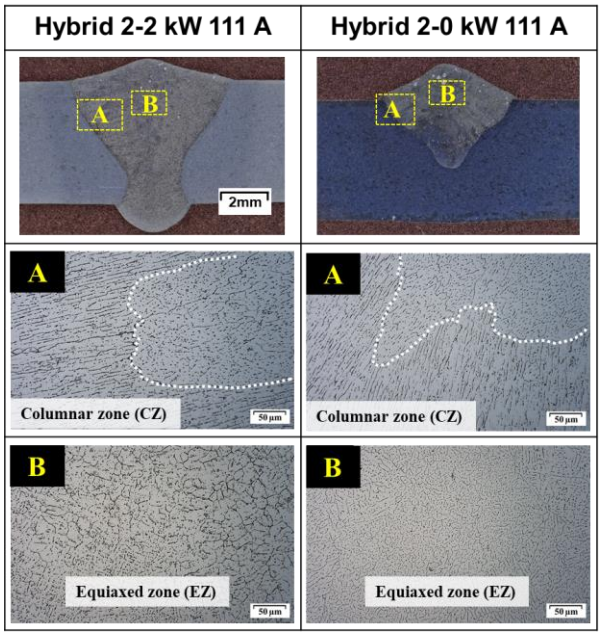

Fig. 3 macro- and micro- structure of dual beam hybrid and core beam hybrid welding.

For an in-depth comparison, the EBSD analysis was conducted. It was obviously observed that the finer equiaxed structure in core beam hybrid than dual beam hybrid as shown in Fig. 4. The average grain size of the dual beam hybrid and core beam hybrid in the central region was measured as 203 μm and 167 μm. Further, it was found that the core beam hybrid showed less level of intensity in the PF result, which means the microstructure has composed of more random crystallographic directions. Not only the grain size, but also the crystallographic direction of the grains has a great influence on the mechanical properties of the material. However, microhardness values that were contrary to the grain size and crystallographic direction were obtained, and it is believed that the difference in the amount of precipitates produced under dual beam hybrid and core beam hybrid had a significant effect.

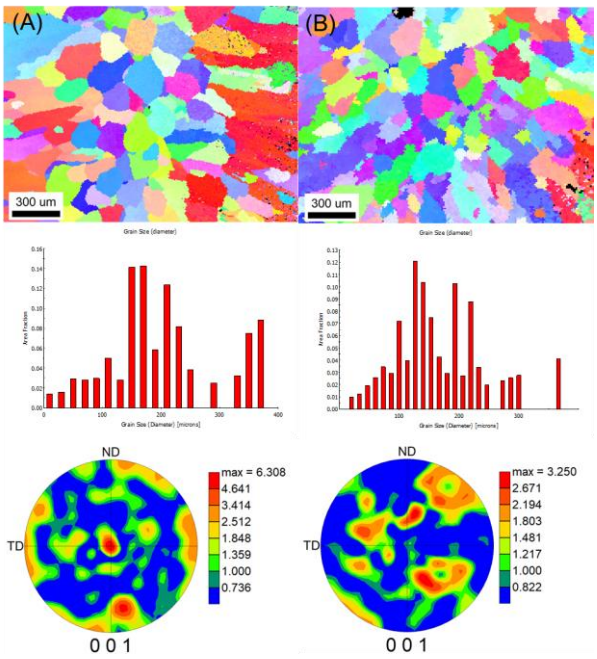

Fig. 4 IPFs of the central region in dual beam hybrid and core beam hybrid were shown in (A) and (B), respecdtively. The grain size charts were shown below it. And the PFs were shown at the bottom.

3.2 Mechanical properties

Fig. 5 presents the micro-hardness distribution of the core beam hybrid and dual beam hybrid welded joint. In the arc-dominated region and the laser-dominated region, the core beam hybrid weld showed lower hardness values than the dual beam hybrid weld. In the HAZ section, the dual beam hybrid also showed higher hardness values than the core beam hybrid. Even though the grain size is larger in the dual beam hybrid, it is believed that the reason these results appear is due to the difference in the amount of precipitates in the weld zone.

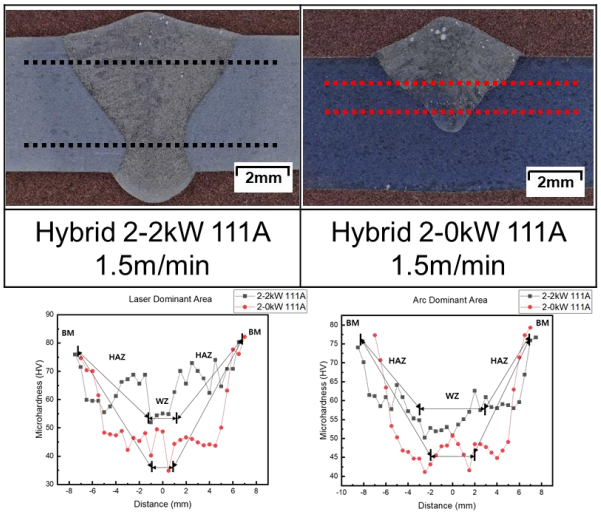

Fig. 5 microhardness of the dual beam hybrid and core beam hybrid welding.

4 Conclusion

In this paper, we discussed the differences in microstructure and mechanical properties for ARM heat

source in ARM laser-arc hybrid welding. Dual beam hybrid welding showed larger grain sizes on average than core beam hybrid welding, and the PF value of dual beam hybrid welding was approximately twice as high as that of core beam hybrid welding. However, dual beam hybrid welding showed higher microhardness values than core beam hybrid welding. This was determined to be a phenomenon that occurred when a large amount of precipitates such as Mg_2Si and Mg_3Si were generated due to the influence of the dual beam.

References

1. J. C. Benedyk, Materials, Design and Manufacturing for Lightweight Vehicles. 79-113, (2010).
2. B. Acherjee, Opt. Laser.Technol. **99**, 60-71, (2018)
3. I. Bunaziv, O. M. Akselsen, X. Ren, B. Nyhus, and M. Eriksson, Metals, **11(8)**, (2021)
4. H. S. Bang, J. H. Kim, J. Weld. Joining, **29(4)**, 27-29, (2011)
5. J. W. Yoon, J.KWS, **18(2)**, 20-26, (2000)
6. K. H. Youn, Y. S. Han, J. KWS, **12(1)**, 16-27, (1994)
7. Y. Kim, S.Kil, J. Weld. Join, **31(2)**, 4-15, (2013)
8. W. V Vaidya, K. Angauthu, M. Koak, R. Grube, and J. Hackius, Welding in the world, **50**, 88-97, (2006)
9. J. F. Tu, A. G. Paleocrassas, J.Mater. Process. Technol, **211(1)**, 95-102, (2011)
10. C.H. Lee, R. W. Chang, J. KWS, **10(3)**, 1-12, (1992)
11. C. H. Lee, R. W. Chang, J. KWS, **11(1)**, 2-8, (1993)
12. C. Zhang, M. Gao, and X. Zeng, Opt. Laser Technol, **120**, (2019)
13. H. Wang, J. Phys.: Conf. Ser, **2185**, (2022)
14. Q. Wang, H. Chen, Z. Zhu, P. Qiu, and Y. Cui, Int J Adv Manuf Technol, **86**, 1375-1384, (2016)